

# Automatika

Journal for Control, Measurement, Electronics, Computing and Communications



ISSN: (Print) (Online) Journal homepage: [www.tandfonline.com/journals/taut20](http://www.tandfonline.com/journals/taut20)

## Smart material selection strategies for sustainable and cost-effective high-performance concrete production using deep learning

T. Seethalakshmi, M. Murugan & P. Maria Antony Sebastin Vimalan

To cite this article: T. Seethalakshmi, M. Murugan & P. Maria Antony Sebastin Vimalan (2024) Smart material selection strategies for sustainable and cost-effective high-performance concrete production using deep learning, *Automatika*, 65:4, 1533-1544, DOI: [10.1080/00051144.2024.2399319](https://doi.org/10.1080/00051144.2024.2399319)

To link to this article: <https://doi.org/10.1080/00051144.2024.2399319>



© 2024 The Author(s). Published by Informa UK Limited, trading as Taylor & Francis Group.



Published online: 10 Sep 2024.



Submit your article to this journal [↗](#)



Article views: 266



View related articles [↗](#)



View Crossmark data [↗](#)



# Smart material selection strategies for sustainable and cost-effective high-performance concrete production using deep learning

T. Seethalakshmi<sup>a</sup>, M. Murugan<sup>a</sup> and P. Maria Antony Sebastin Vimalan<sup>b</sup>

<sup>a</sup>Department of Civil Engineering, Government College of Engineering, Tirunelveli, India; <sup>b</sup>Department of Civil Engineering, PSN College of Engineering and Technology, Tirunelveli, India

## ABSTRACT

The creation of high-performing concrete (HPC) is greatly influenced by the selection of materials, with cost and sustainability factors playing a bigger part in contemporary building techniques. To overcome these limitations, we developed a Multi-Objective Ant Colony Adaptive Dense Convolutional Neural Network (MOAC-ADenseNet) with 5-K-Fold cross validation, a dependable and precise forecasting model for the cost-effective selection of HPC material. First, we collect a concrete material dataset for evaluating the suggested method. MOAC-ADenseNet utilized Dense convolutional neural networks and ant colony optimization for complex material data analysis, which makes it easier to choose expensive and sustainable materials for high-performance concrete manufacturing operations. The experimental findings of the suggested approach are evaluated for the relative measure such as Pearson's Linear Correlation Coefficient (R) is 0.93, the Root Mean Square Error (RMSE) is 91.38, Mean Absolute Error (MAE) of 58.15, and Mean Absolute Percentage Error (MAPE) is 8.79. The outcomes demonstrated that the material cost of HPC was correctly predicted by the MOAC-ADenseNet. The actual measured value and the MOAC-ADenseNet model predictions, following 5-K-fold cross-validation and input feature improvement, shows its effectiveness. A The MOAC-ADenseNet approach provides feasible method for enhancing material selection in HPC manufacturing accomplishing sustainability and cost-effectiveness goals.

## ARTICLE HISTORY

Received 11 April 2024  
Accepted 26 August 2024

## KEYWORDS

Concrete material; high-performing concrete (HPC); multi-objective ant colony based adaptive dense convolutional neural networks (MOAC-ADenseNet)

## 1. Introduction

The requirement for durable and high-strength materials is growing to improve the sustainability of civil infrastructure [1]. The increased fibre and cementitious concrete known as ultra-high-performing concrete (UHPC) have high compressive strength (120–250MPa), tensile strength (15–20MPa), and exceptional durability. Its particle packing density is 0.825–0.855. UHPC has three to 16 times the compressive force of ordinary concrete and 300 times flexibility and absorption of energy of HPC [2]. UHPC was regarded as the ideal material for seismic design purposes because of its exceptional mechanical properties, excellent ductility and durability under strain. Improving the long-term durability of structures and infrastructure facilities is conceivable using UHPC [3]. UHPC's increased durability could be helpful for infrastructure that was subjected to extreme environmental loads [4]. Utilizing UHPC also results in shorter construction times, less labour and equipment necessary for the construction of precast elements and net area by reducing the quantity of concrete required in a project. However, UHPC has a high packing density and lacks a coarse aggregate, it contains a large amount

of concrete, quartz sand, quartz powder and silica fume, which raises the cost of UHPC and it has a significant negative environmental effect [5]. The construction industry is increasingly examining smart material selection techniques to optimize UHPC manufacturing processes in response to the rising need for sustainable building practices.

### 1.1. Significance of smart construction material (SCMs) selection techniques

It is promising to use smart construction materials (SCMs) for structural health monitoring in construction and civil infrastructure [6] that can detect damage and self-stress. SCMs are anticipated to address the drawbacks of existing monitoring systems that use widely attached or embedded sensors connected by wire to data collecting systems, such as their poor durability, high cost and limited capacity for localized sensing [7]. By using fine steel slag aggregates (FSSAs), smart high-performance concrete (S-UHPC) can sense compressive stress up to 60 MPa, demonstrating impressive self-stress capabilities. Applying the S-UHPC to the tendons' anchoring zone would allow to

**CONTACT** P. Maria Antony Sebastin Vimalan ✉ [vimalan14@gmail.com](mailto:vimalan14@gmail.com) 📍 Department of Civil Engineering, PSN College of Engineering and Technology, Tirunelveli, Tamilnadu 627152, India

© 2024 The Author(s). Published by Informa UK Limited, trading as Taylor & Francis Group.

This is an Open Access article distributed under the terms of the Creative Commons Attribution-NonCommercial License (<http://creativecommons.org/licenses/by-nc/4.0/>), which permits unrestricted non-commercial use, distribution, and reproduction in any medium, provided the original work is properly cited. The terms on which this article has been published allow the posting of the Accepted Manuscript in a repository by the author(s) or with their consent.

track the reduction in stretching force in prestressing steel (PS) structures. The measurement of the related resistance to power of the S-UHPCs with steel fibres supported the effective identification of fractures or other damage inside tensile samples of S-UHPCs under direct stress [8].

### 1.2. Challenges of UHPC production

The UHPC has several advantages, but several production-related issues need to be resolved for sustainability and economy [9]. The selection of appropriate materials, such as cement, aggregates, mixtures and SCMs is one of the main issues. The lifetime and performance of UHPC structures are strongly influenced by the quality, availability and environmental effects of these materials. Sustainable manufacturing methods are necessary since the manufacturing process may contribute to waste creation, resource depletion and carbon emissions [9]. The goal is to create an accurate and dependable forecasting model MOAC-ADenseNet for the cost-effective selection of HPC materials. It is accomplished by combining deep learning and multi-objective optimization techniques to integrate sustainability and economic factors.

### 1.3. Contribution of the study

- The study created a cutting-edge model for cost-effective material selection in the manufacturing of HPC called MOAC-ADenseNet.
- The article MOAC-ADenseNet to accomplish the important goal of UHPC issues by accurately predicting material costs.
- The study used ant colony optimization for optimization problems and dense convolutional neural networks for complex material data analysis, improving selection efficiency.
- The study improves the selection of materials used in the production of HPC, thereby fulfilling the objectives of cost- and sustainability-effectiveness in HPC.

The article's structure is explained in the following manner. Section 2 of this study reviews the relevant literature. The dataset and suggested methodology are described in Section 3. Sections 4 explain the findings and discussion of the research. Finally, Sections 5 give findings at the end of this investigation.

## 2. Related work

The article [10] provided measures and instruments for assessing the structural efficiency, price and carbon dioxide (CO<sub>2</sub>) emissions of mixes of concrete. Due to popular assumptions, durability and performance can be maximized in concrete with a high binder composition and ultra-high strength. Through

a multi-objective approach utilizing Bayesian optimization Random Forest (BO-RF) and non-dominated sorting genetic algorithm (NSGA-III), the study [11] optimized concrete cost and performance in hostile conditions, producing precise forecasts and thorough mix proportions for increased durability. The study [12] improved the development of UHPC by utilizing AI approaches. It delivers accurate design, better prediction and user-friendly software, via the use of an artificial neural network (ANN) based on genetic algorithms (GA) and the Modified Andreasen and Andersen system. The research [13] created geopolymer materials fine-grained cement for sustainable building that was both cost-effective and ecologically beneficial. Considerable increases in properties of strength have been achieved by adjusting the quantity of the activator and the temperature of treatment, indicating that the approach has the potential to be widely used. To optimize the proportions of a HPC mix, the research [14] integrated the RF, least-squares support vector machine (LSSVM), and NSGA-II methods into a hybrid smart framework. For durable and affordable concrete formulations, it detects important variables, forecasts performance and accomplishes multi-objective optimization.

The research [15] described an Artificial Intelligence (AI)-driven strategy for automatically identifying UHPC that was low-carbon and economical. It reduces the impact on the environment and material costs by combining many-objective optimization, automated neural networks and generative modelling. An automated technique to acquire concrete design data from publications was developed in the study [16] which improved Machine learning (ML)-based creation of low-carbon, economical UHPC. In time, the optimization efficiency and accuracy of prediction of the approach are enhanced by its self-updating process. The research [17] developed sophisticated forecasting algorithms that include both mechanical and environmental factors for high-strength fibre-reinforced concrete beams. All of the existing strategies are accurate; the Bayesian neural network (BNN) model executes most effectively and provides comprehensive design insights. The research [18] optimized the proportions of the UHPC combination for cost, carbon emissions and fundamental features. Using the analytical hierarchy process and ML, suggests a well-balanced UHPC formulation for broad use. The paper [19] created AI-based instruments for assessing how the structure of the mixture of concrete impacts cost, eco-efficiency and mechanical durability. The results contradict industry norms by demonstrating that high-strength concrete solutions significant for cost or environmental efficiency. The study [20] used AI-guided algorithms to identify low-cost, low-carbon UHPC. Significant cost of materials and life-cycle carbon footprint decreases are possible with the integration of automated ML and generative modelling. The research [21] examined the

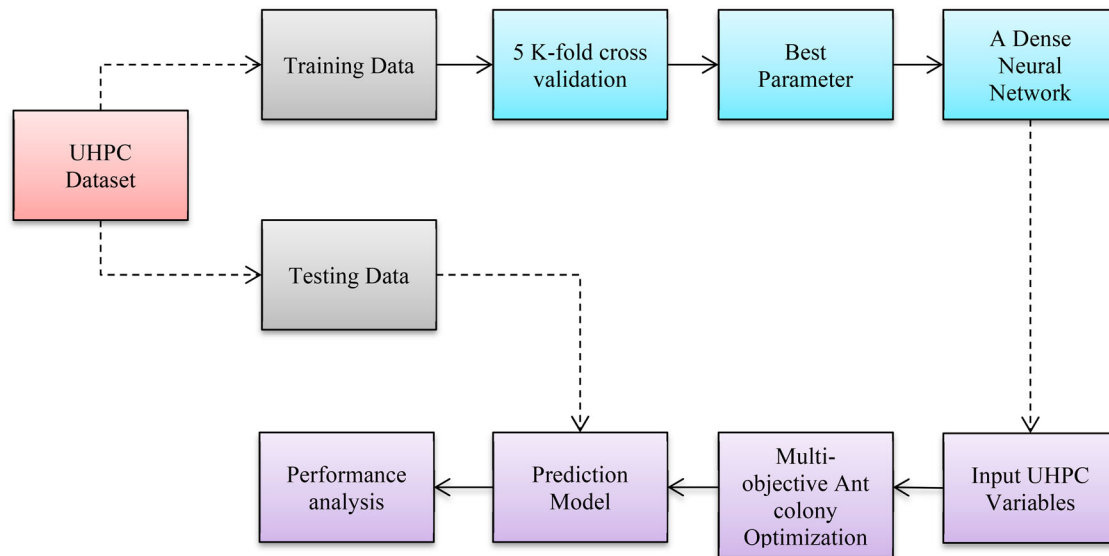


**Figure 1.** Overview of proposed methodology.

application of nanoparticles in concrete to improve its mechanical qualities and solve environmental and financial issues. Improved performance, robustness, sustainability and financial viability are shown by the results. Concrete self-healing solutions in response to the effects of climate change are thoroughly examined in the paper [22]. It highlighted the possibility for increased sustainability, a longer lifetime and lower maintenance costs by analyzing materials, techniques and environmental factors.

This study fills a gap in the literature by concentrating on concrete performance, cost and environmental impact from a different perspective. By combining deep learning models with sophisticated optimization approaches, our study provides a comprehensive method to improve UHPC's sustainability and cost-effectiveness. Our method fills a critical gap in the development of balanced, high-performance and environmentally friendly concrete formulations by combining multi-objective optimization with state-of-the-art AI approaches, in contrast to prior works that either maximize specific properties or employ conventional methods.

### 3. Proposed methodology

The current study established a framework for choosing the cost-effective HPC material while taking cost and environmental sustainability under extremely non-linear restrictions by utilizing the capabilities of the MOAC-ADenseNet approaches. Figure 1 provides an overview of the study's approach.

#### 3.1. Data acquisition

The model was changed in this study using an overall of 931 instances of HPC materials. The 701 findings from

scientific journals can provide additional information regarding the database [23] and consulting experimental activities use internal experimental data to perform thorough analysis and improve the model. The data set is divided into two sets, train set 80% of the entire dataset and a validation set 20%.

#### 3.2. 5-K-fold validation

By dividing the data set into five groups, training the model on four of the subsets, and iteratively validating it on the fifth, the study used 5-K-Fold cross-validation to evaluate the model's performance resilience. The flow chart in Figure 2 illustrates how the k-fold cross-validation begins with the data being randomly divided into K groups. Each group is then subjected to the subsequent actions are performed,

- The testing dataset should be selected from among the training folds.
- A training set consisting of the remaining  $K-1$  categories is employed.
- Model training and evaluation should be performed with the chosen training dataset and testing dataset.

Typically,  $k$  in the limited dataset of this study is set to 5, an empirical value derived from numerous experimental trials. When MOAC-ADenseNet simulation is used directly, the outcome has minimal volatility and little bias. Furthermore, a distinct testing fold ranging from  $D1$  to  $D5$  was consistently chosen as the verification set. These five data sets were systematically entered into the MOAC-ADenseNet model. Using 5-time cross-validation, the model evaluation error resulting from the unintentional partitioning of the sample can be eliminated.

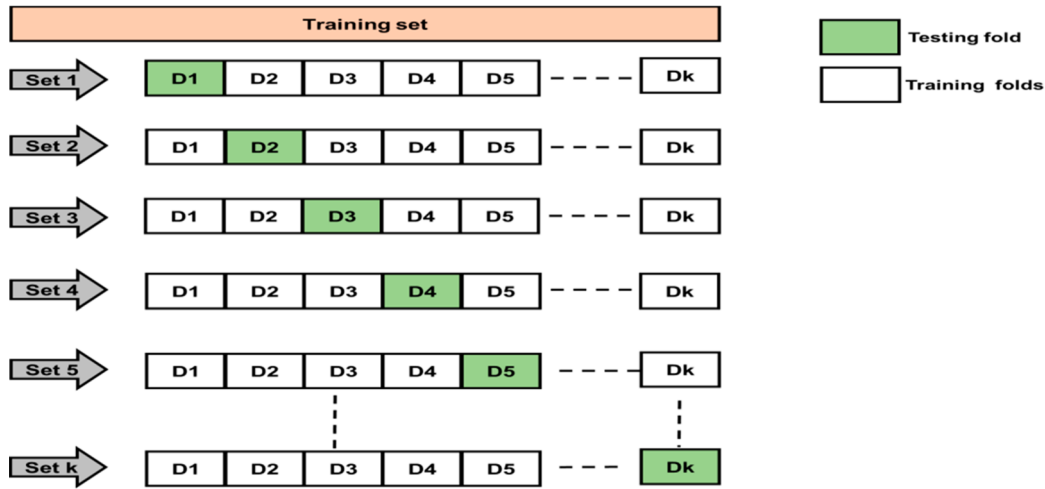


Figure 2. 5-K-Fold cross validation.

### 3.3. Multi-objective ant colony-based adaptive dense convolutional neural networks (MOAC-ADenseNet)

We improve concrete material selection for sustainable and economical HPC manufacturing using MOAC-ADenseNet. The smaller parameters, ADenseNet is a state-of-the-art CNN framework considered for cost-effective HPC recognition. For HPC to be produced sustainably and economically while maintaining environmental responsibility, it is essential to select concrete materials. Combining mathematical models and data-driven insights, the adaptive dense convolutional neural networks (ADenseNet) can improve the material selection procedure. ADenseNet is comparable to ResNet with several key variations. ResNet uses an additive attribute (+) to mix that came before with the future layers, whereas ADenseNet uses its concatenated (.) attributes to integrate the output of the prior layer with a future layer. The goal of the ADenseNet Architecture is to solve this issue of cost-effective HPC by strongly coupling every layer [24]. The DenseNet-121 [5 + (6 + 12 + 24 + 16) × 2] = 121]framework, one of the several ADenseNet models contains DenseNet (121), (160), (201). Various DenseNet-121 details: 5 layers are for convolution and pooling, 3 are for transition layers (6, 12, 24), 1 is for classification layer (16), and 2 is for dense block (1 × 1 and 3 × 3 conv.) for material selection for producing sustainable, cost-effective and HPC. Conventional CNNs typically compute the output layers ( $k^{th}$ ) by applying a transformation that is not linear  $G_k(\cdot)$  to the previous layer's output ( $W_{k-1}$ ) represent in equation (1).

$$W_k = G_k(W_{k-1}) \quad (1)$$

ADenseNets output layer capability maps should be concatenated with the inputs instead of adding them together. A simple communication mechanism for improving information movement among layers is provided by ADenseNet. The characteristics of all

earlier layers provide inputs to the  $l$ th layer shown in equation (2).

$$W_k = G_k[(W_0, W_1, W_2, \dots, W_{k-1})] \quad (2)$$

#### 3.3.1. Dense block

Where the output maps of earlier layers are concatenated to produce a single tensor,  $[W_0, W_1, W_2, \dots, W_{k-1}]$ . Among the functions, the non-linear transformation function is represented by  $G_k(\cdot)$ . Three main processes make up this function, pooling and convolution (CONV), activation (ReLU) and batch normalization (BN) [25–27]. Figure 3 illustrates the architecture of ADenseNet. But the growth rate  $l$  does in the following ways to help generalize the  $k^{th}$  layer:  $l^{[k]} = (l^{[0]} + l(k - 1))$ . Where the number of connections is expressed as  $l^{[0]}$ . These  $l$  feature maps, which are produced by each dense block, can be intuitively seen as their local states, which concatenate to contribute to the worldwide state of the network.

#### 3.3.2. Transition layers

Since only map features of the same size can be combined, adaptive dense blocks are unaffected by feature size-down sampling. A crucial component of CNNs is down sampling [28]. To accomplish this, dense blocks are connected by transition layers with pooling, creating an ADenseNet. The BN – ReLUConv(1 × 1) with Average Pooling (2 × 2) is the fundamental design of the transition layer [29].

#### 3.3.3. Composite function

The  $G_k(\cdot)$  is the combination function of three successive operations: a 3 × 3 Conventional, a ReLU, and BN.

#### 3.3.4. Pooling layers

When feature maps fluctuate in size, Equation (2)'s concatenation procedure becomes unworkable. However, convolutional networks require layers of down-sampled

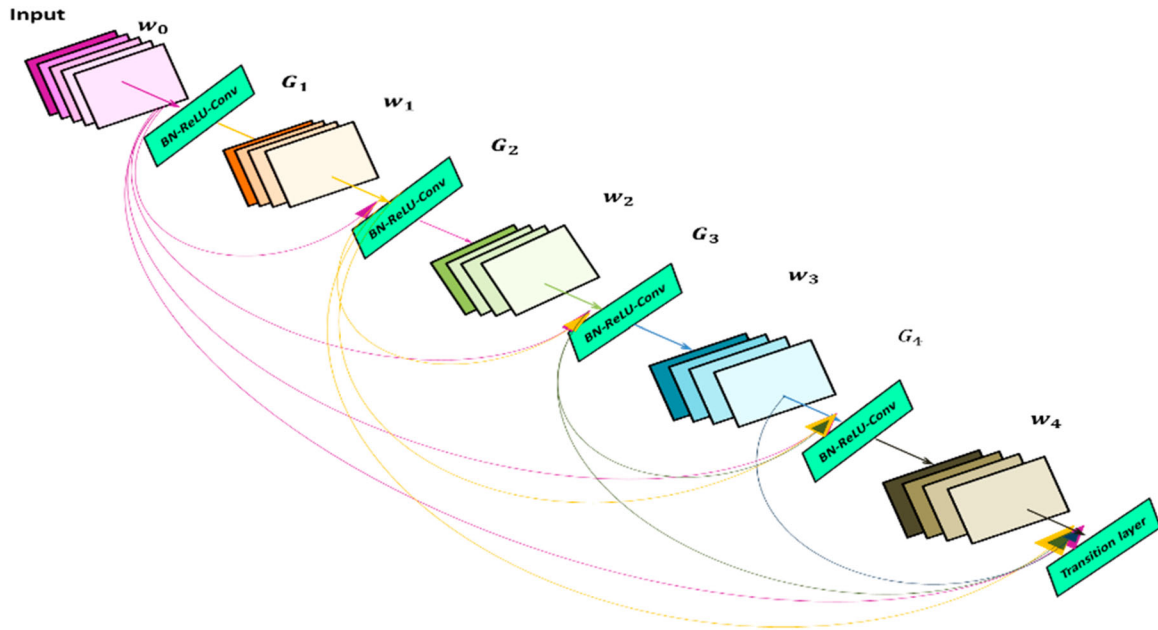


**Figure 3.** Architecture of ADenseNet.

data to change the dimensions of the feature maps. The framework segments the system into several tightly connected blocks to enable down sampling. Transition layers are the layers that perform pooling and convolution in between blocks. It employed transition layers that comprised of a batch normalization layer, an  $2 \times 2$  average pooling layer and a  $1 \times 1$  convolutional layer [30]. The categorical cross-entropy loss function is the loss function to reduce classification mistakes; the model is guided by this function, which calculates the difference between the true class labels and the predicted class probabilities, when used to solve multi-class classification issues.

### 3.3.5. Growth rate

The  $k^{th}$  layer has  $l^{[k]} = (l^{[0]} + l(k - 1))$  input feature maps if each function  $G_k$  generates  $l$  feature maps, where  $l^{[0]}$  is the input layer's channel count. ADenseNet differs significantly from current network topologies that can contain extremely narrow layers, such as  $l = 12$ . The hyperparameter  $k$  is referred to the network's growth rate. The rate of growth controls the quantity of new data that every layer advances the overall condition. Different from conventional network topologies, it is not necessary to duplicate the global state from layer to layer once it is written because it can be accessed from anywhere in the network. ADenseNet's dense connection structure allows to capture complex interactions between different material attributes, which are used in material selection for the production of concrete. It can manage complex data patterns extremely well. Due to its versatility and resilience, ADenseNet is an effective tool for examining a variety of datasets in different applications.

Utilizing the effective and adaptive search capabilities inspired by the collective behaviour of ants, the

multi-objective ant colony (MOAC) approach is used for HPC production because it can simultaneously optimize conflicting objectives like sustainability, cost-effectiveness and performance in material selection. An effective way to address the intricate and multi-faceted problems associated with intelligent material selection methods for concrete production is provided by this integration, which combines the advantages of MOAC with the flexibility and resilience of ant colony algorithms. Due to their higher-order structures, series controllers are widely used. The following equation (3) defines the transfer function for HPC production in a continuous system.

$$h_d(o) = L_o + \frac{L_j}{t} + L_c t \quad (3)$$

Based on the design, the constants  $L_o$ ,  $L_j$ , and  $L_c$  must be determined to achieve the necessary performance requirements. The continuous-time HPC production model is used in equation (4).

$$\begin{aligned} f(s) &= q(s) - z(s), v(s) \\ &= L_o f(s) + L_j \int_0^s f(\tau) d\tau + L_c f(s) \\ &= v_o(s) + v_j(s) + v_c(s) \end{aligned} \quad (4)$$

Where the distinction between the reference signal,  $q(s)$ , and the regulated process's output,  $z(s)$ , is represented as  $f(s) = q(s) - z(s)$ . In addition to lowering or eliminating the material cost and SteadyState error, the use of HPC production aims to enhance dynamic response. To calculate the transient response performance indices, such as rise time ( $s_q$ ), overshoot ( $P_t$ ), settling time ( $s_t$ ) and integral square error ( $ISE$ ), to evaluate the efficiency of the HPC production systems.

It would be preferable to express our optimization problem as a construction graph to maximize the advantage of the ACO algorithm. The number of individuals is represented by a  $100 \times 3$  matrix, and the ants use the objective function  $LA$  to minimize in selecting the optimal parameters  $L_o, L_j$  and  $L_c$  of the material selection system. Each of the three study parameters  $L_o, L_j$  and  $L_c$  is represented by 100 numbers, or nodes. Consequently, the ideal values of the parameters  $L_o, L_j$  and  $L_c$  are represented by a single node. Selecting the optimization concrete material criteria that are used to fit the first stage of optimization approach. It can integrate multiple indexes of the transient response performance of the HPC production into a single objective function that is made up of the weighted sum of the objectives. The objective function needs to be specified in equation (5).

$$K^B = \min(\Phi E) \quad (5)$$

Where  $E$  is equal  $[E_1 E_2 E_3 E_4 E_5 E_6 E_7]$ ,  $S$  represents the vector of objective functions;  $E_1$  denotes the setting time ( $s_q$ ),  $E_2$  represents overshoot ( $P_t$ ),  $E_3$  represents rise time ( $s_t$ ),  $E_4$  reflects integral absolute error (IAE),  $E_5$  symbolizes integral square error (ISE),  $E_6$  represents integral time absolute error (ITAE),  $E_7$  represents integral time square error (MSE), and  $\Phi = [\lambda_1 \lambda_2 \lambda_3 \lambda_4 \lambda_5 \lambda_6 \lambda_7]$ , vector of nonnegative weights. Concrete material challenges request to identify the optimal trade-off between several, competing goals. There will be multiple solutions that optimize the objectives at the same time when considering all the objectives in these situations and none of these solutions appears better than the other. In most cases, no single optimal solution outperforms the others about all objectives. As a result, the Pareto front presents with a collection of solutions that are superior to residual answers. Solutions that fall inside the Pareto front among the workable solutions are referred to nondominated solutions and the remaining options are referred to be dominated. Since none of the Pareto-set solutions is naturally superior to the other non-dominant options, they are all equally acceptable in terms of achieving all of the goals. MOAC builds possible good solutions using the pheromone matrix  $\tau = \{\tau_{ji}\}$ .  $\tau_{ji} = \tau_0$  for all  $(j, i)$  is the initial value of  $\tau$ , where  $\tau_0 > 0$ . Equation (6) defines the probability  $PA_{ij}(t)$  of selecting a material node  $i$  at node  $j$ . Beginning at the source node, the ant uses (6) to build a comprehensive solution at each iteration of the algorithm.

$$O_{ji}^B(s) = \frac{[\tau_{ji}(s)]^\alpha [\eta_{ji}]^\beta}{\sum_{j,i \in S^B} [\tau_{ji}(s)]^\alpha [\eta_{ji}]^\beta} \text{ if } j, i \in S^B \quad (6)$$

Where  $\eta_{ji}$  stands for heuristic functions,  $\alpha$  and  $\beta$  are constants that indicate how much the pheromone values and the heuristic values influenced the ant's decision, and  $S^B$  is the path that the ant  $B$  selected at a particular moment. There is a method to prevent an

infinite growth in pheromone paths, pheromone evaporation. Additionally, poor decisions are illustrated in equation (7).

$$\tau_{ji}(s) = \rho \tau_{ji}(s-1) + \sum_{B=1}^{NA} \Delta \tau_{ji}^B(s) \quad (7)$$

Where  $\rho$  is the evaporation rate ( $0 < \rho \leq 1$ ),  $NA$  is the number of ants and  $\Delta \tau_{ji}^B$  is the number of pheromones on each path. Algorithm 1 creates an empty Pareto set for the best solutions while initializing heuristic matrices and pheromone trails. It assesses pathways iteratively, updating the optimal answer and removing dominating ones according to probability. It directs material selection towards high-performance, economically viable, and sustainable concrete production by iteratively evaluating weighted objectives and updating pheromone trails, ultimately returning the optimal solution and Pareto set.

---

**Algorithm 1:** Multi-objective Ant Colony Optimization (MOACO)

---

**Initialize:** Pheromone trails  $\tau(\tau^l)$ , heuristic matrix  $\eta(\eta^l)$ , Pareto set  $O_s = \phi$   
**Determine** the weights for each objective (e.g., randomly)

**Begin**

**While** (the stopping criteria are NOT met) do

**For** each path

**Evaluate** the probability of take

**Update** the best solution and remove the dominant ones

**End for**

**For** each objective

**Evaluate** the weighted sum of objectives

**Determine** the best solution

**Update** the Pheromone trails

**End for**

**End while**

**Return**  $ND$  and  $O_s$

**End**

---

Using the complementing strengths of MOAC-ADenseNet is a promising method for forecasting cost-effective HPC materials. It is intended to be used for optimization problems in the areas of material-technical and scientific. Its potential is found in its capacity to better decision-making processes by offering observations into the trade-offs between various goals, which makes informed and optimal material selection possible in a variety of applications.

#### 4. Result and discussion

This section begins with a discussion of each network's training process. Next, a comparison is made between the conventional method. The suggested MOAC-ADenseNet approach was performed by creating Microsoft Excel macro code on a PC equipped with an Intel 3.20 GHz processor and 8 GB of RAM.

A large collection of UHPC was gathered for this study from [23]. However, the raw database has several problems, including notable data imbalance and significant gaps in the experimental data. For example, only 27 mixes had the component metakaolin and 59 mixtures

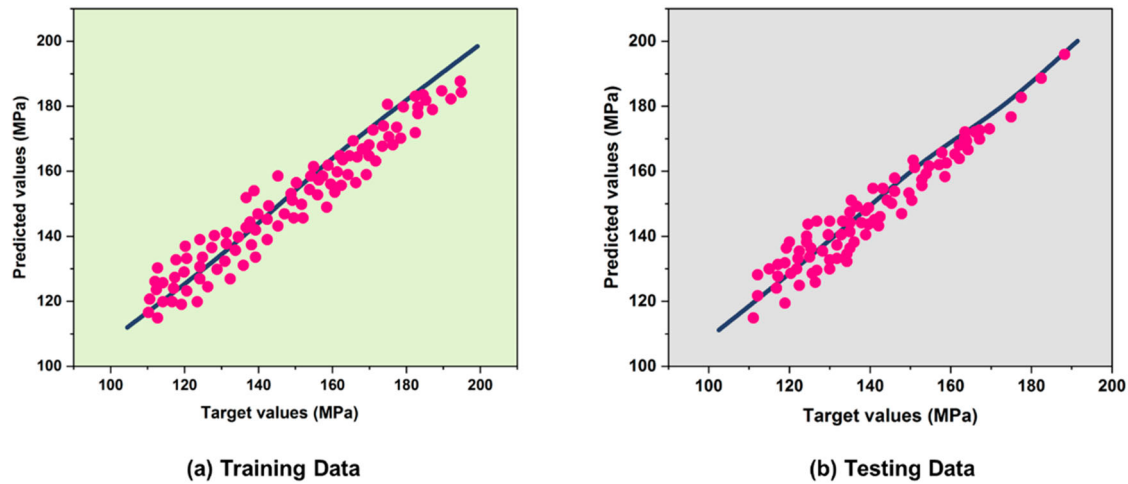


**Figure 4.** Testing and training subgroups.

contained husks of rice ash. To ensure the durability and dependability of the dataset, a preprocessing phase was performed to address these problems. This phase included a systematic elimination of anomalies and the removal of values-containing records that were missing. As a result, 540 UHPC data formed the final dataset. Nineteen design factors comprised the input variables; these were listed in Table 1. 19 of the input factors listed below were chosen: “Cement (C), fly ash (FA), silica fume (SF), ground granulated blast-furnace slag (GGBFS), recycled glass powder (GP), rice husk ash (RHA), fluid catalytic residue (FC3R), metakaolin (MK), limestone powder (LP), water (W), high-range water-reducer superplasticizer (HRWR), quartz powder (QP), the maximum size of aggregate (MSA), water to binder ratio (WB), water to total powders ratio (WP), total aggregate (A), and virtual packing density (VPD)”. To tackle the constraints caused by the models’ low learning rates at high elements, the input variables are adjusted to fall between 0 and 1. This scaling helps to mitigate concerns linked to variable size differences by ensuring that all inputs contribute equally to the model’s learning process. After that, the adjusted information is divided into two sets: a train set that covers 80% of the entire dataset and a validation set that covers 20%. Figure 4(a) and (b) illustrate the regression graphs for the training and test datasets, which are the two subsets.

The training samples are progressively selected as the input information using the 5-K-fold cross-validation approach. Next, the MOAC-ADenseNet system is employed to select the most cost-effective UHPC smart material.

#### 4.1. Validity

The outcomes of the 5-K-fold cross-validation process for various datasets are shown in the Table 2. In this stage, the evaluation metrics are compared to assess which model has the best prediction performance.

**Table 1.** Input variables.

| Material        | Input Variables |        |            |          |
|-----------------|-----------------|--------|------------|----------|
|                 | Min             | Max    | Mean       | SD       |
| C $m^3/m^3$     | 0.120           | 0.530  | 0.267      | 0.062    |
| SF $m^3/m^3$    | 0.000           | 0.155  | 0.048      | 0.040    |
| FA $m^3/m^3$    | 0.000           | 0.250  | 0.017      | 0.044    |
| GGBSF $m^3/m^3$ | 0.000           | 0.247  | 0.007      | 0.025    |
| GP $m^3/m^3$    | 0.000           | 0.202  | 0.026      | 0.051    |
| RHA $m^3/m^3$   | 0.000           | 0.177  | 0.004      | 0.018    |
| FC3R $m^3/m^3$  | 0.000           | 0.091  | 0.004      | 0.013    |
| MK $m^3/m^3$    | 0.000           | 0.161  | 0.002      | 0.013    |
| LP $m^3/m^3$    | 0.000           | 0.190  | 0.024      | 0.043    |
| W $m^3/m^3$     | 0.103           | 0.364  | 0.200      | 0.034    |
| HRWR $m^3/m^3$  | 0.017           | 0.042  | 0.027      | 0.005    |
| QP $m^3/m^3$    | 0.000           | 0.235  | 0.027      | 0.052    |
| MSA $\mu m$     | 0.000           | 19,000 | 1765.970   | 2580.085 |
| WB (ratio)      | 0.124           | 0.322  | 0.189      | 0.036    |
| WP (ratio)      | 0.107           | 0.322  | 0.177      | 0.034    |
| A $m^3/m^3$     | 0.000           | 0.649  | 0.34585408 | 0.117    |
| VPD (ratio)     | 0.609           | 0.877  | 0.774      | 0.041    |
| CS MPa          | 100             | 214    | 143.464    | 21.925   |

Note: Max = Maximum, SD = Standard Deviation and Min = Minimum.

**Table 2.** Result of 5-K-Fold Cross validation of MOAC-ADenseNet.

| Metric | 1      | 2      | 3      | 4      | 5     |
|--------|--------|--------|--------|--------|-------|
| MAE    | 8.068  | 5.622  | 7.083  | 6.838  | 4.737 |
| RMSE   | 10.094 | 24.294 | 18.024 | 8.988  | 7.145 |
| MAPE   | 28.175 | 17.408 | 18.787 | 46.888 | 18.47 |
| R      | 0.876  | 0.868  | 0.879  | 0.843  | 0.979 |

Some test groups score worse in both the RMSE and MSE measures and the results perform worse, while having correlated values closer to 1.

The results of the K-fold cross-validation, which are displayed in Table 4, indicate that group 5 should be the best model because its R, MAE, RMSE and MAPE values.

#### 4.2. Performance evaluation

In this section, we compare the performance of the current approach and the proposed MOAC-ADenseNet



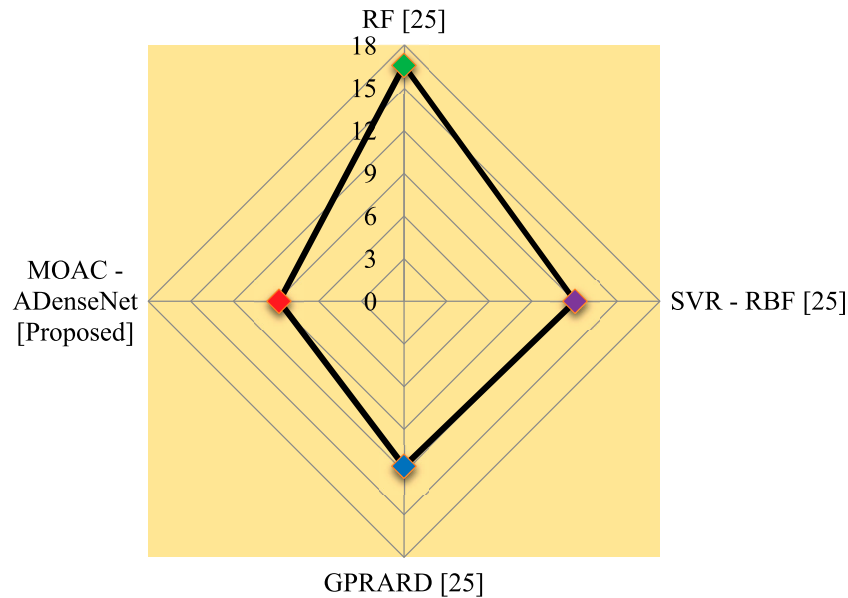


**Figure 5.** Result of MAPE.

**Table 3.** Values of MAPE.

| Methods                     | MAPE  |
|-----------------------------|-------|
| RF [31]                     | 16.58 |
| SVR – RBF [31]              | 12.03 |
| GPRARD [31]                 | 11.6  |
| MOAC – ADenseNet [Proposed] | 8.79  |

method using metrics: the mean absolute percentage error (MAPE) and Pearson's linear correlation coefficient (R) as relative measures, and the root mean square error (RMSE) and mean absolute error (MAE). The traditional methods like Support Vector Regression with Radial Basis Function kernel (SVR-RBF) [31], Random Forest (RF) [31] and Gaussian process regression Automatic Relevance Determination (GPR ARD) [31].

#### 4.2.1. Mean absolute percentage error (MAPE)

MAPE is assessing forecasting model or prediction accuracy in cost-effective UHPC material selection. The absolute percentage inaccuracy is averaged to calculate it. Equation (8) for MAPE. Figure 5 and Table 3 represent the comparison outcome of the suggested method. The MOAC-ADenseNet method attains 8.79, while current methods like RF obtained 16.58, GPRARD obtained 11.60 and SVR-RBF obtained 12.03. The MOAC-ADenseNet approach is very useful for cost-effective UHPC material selection.

$$MAPE = \frac{100}{N} \sum_{H=1}^N \left| \frac{c_h - p_h}{c_h} \right| \quad (8)$$

#### 4.2.2. Mean absolute error (MAE)

A model employed in the material selection process is measured by MAE, which estimates the average absolute variance between its actual values and anticipated. MAE is calculated using the following equation (9).

**Table 4.** Numerical values of MAE.

| Methods                     | MAE   |
|-----------------------------|-------|
| RF [31]                     | 93.53 |
| SVR – RBF [31]              | 68.25 |
| GPRARD [31]                 | 63.25 |
| MOAC – ADenseNet [Proposed] | 58.15 |

**Table 5.** Comparison values of RMSE.

| Methods                     | RMSE   |
|-----------------------------|--------|
| RF [31]                     | 129.05 |
| SVR – RBF [31]              | 109.32 |
| GPRARD [31]                 | 95.98  |
| MOAC – ADenseNet [Proposed] | 91.38  |

The proposed method is compared to current methods, shown in Figure 6 and Table 4. The suggested MOAC-ADenseNet strategy (58.15) has lower numerical results while compared to an existing method like RF has 93.53, GPRARD has 63.25 and SVR-RBF has 68.25. The MOAC-ADenseNet has a significant effect on cost-effective UHPC material selection.

$$MAE = \frac{1}{n} \sum_{H=1}^N |c_h - p_h| \quad (9)$$

#### 4.2.3. Root mean absolute percentage error (RMSE)

The difference between concrete material cost values predicted by the model ( $ok$ ) and the actual concrete material cost observed (measured) values ( $dk$ ) is quantified by the RMSE. It is an indicator of the model's overall correctness. Equation (10) is used for calculating RMSE. Figure 7 and Table 5 shows the comparison result. The suggested method achieved 91.38 while compared to the current approaches (RF –129.05, GPRARD –95.98 and SVR-RBF –109.32). As a result, the proposed method has lower values than existing methods, which indicates the MOAC-ADenseNet

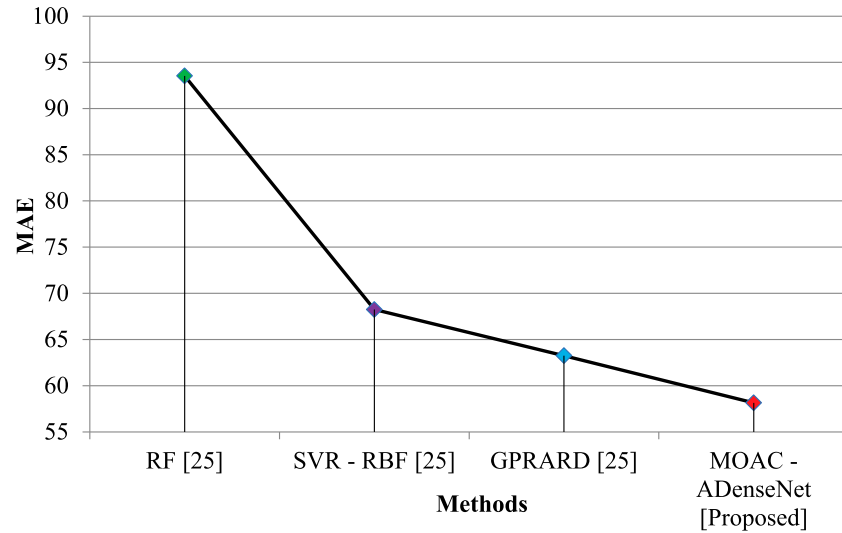


Figure 6. Result of MAE.

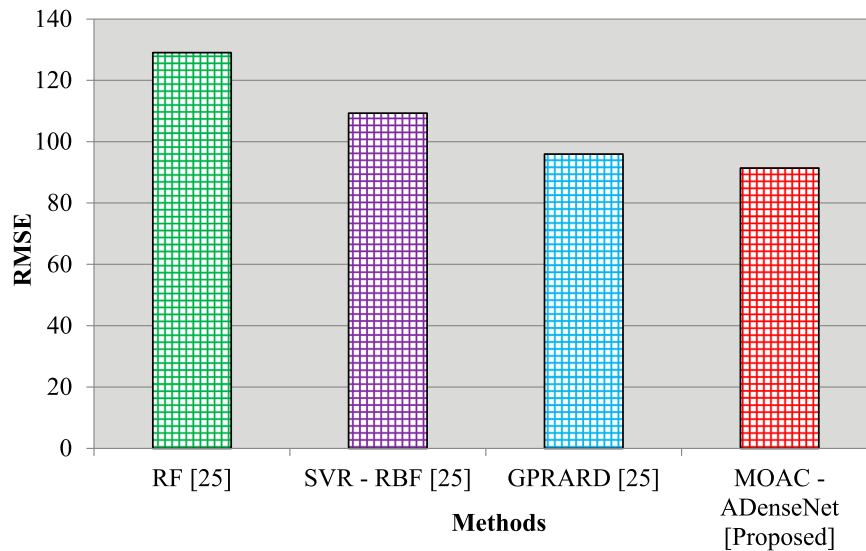


Figure 7. Comparison result of RMSE.

Table 6. Values of R.

| Methods                     | R    |
|-----------------------------|------|
| RF [31]                     | 0.79 |
| SVR - RBF [31]              | 0.86 |
| GPRARD [31]                 | 0.89 |
| MOAC - ADenseNet [Proposed] | 0.93 |

gives a better performance result of cost-effectiveness in UHPC.

$$RMSE = \sqrt{\frac{1}{n} \sum_{H=1}^N (c_h - p_h)^2} \quad (10)$$

#### 4.2.4. Pearson's linear correlation coefficient (R)

The linear correlation coefficient ( $R$ ) quantifies the relationship between the values that the model  $p_h$  predicts and the actual values that are seen (measured), or  $c_h$ . Equation (11) for  $R$  [32, 33]. Figure 8 and Table 6 show the comparison result of the suggested method. The MOAC-ADenseNet achieved a greater result (0.93)

than existing methods (RF-0.79, GPRARD -0.89, and SVR-RBF -0.86).

$$R = \frac{\left[ \sum_{H=1}^N (c_h - \bar{c})(p_h - \bar{p}) \right]^2}{\left[ \sum_{H=1}^N (c_h - \bar{c})^2 \right] \left[ \sum_{H=1}^N (p_h - \bar{p})^2 \right]} \quad (11)$$

where  $H = 1, 2, \dots, N$  is the number of cases in the collection and represents the mean of and the mean of  $oc_h$ .

#### 4.3. Discussion

While SVR-RBF, RF and GPRARD are effective methods for modelling intricate relationships and producing predictions, each has disadvantages when it involves selecting materials for UHPC that are affordable. While strong against overfitting and adaptable, RF [31] might not be able to capture the intricate

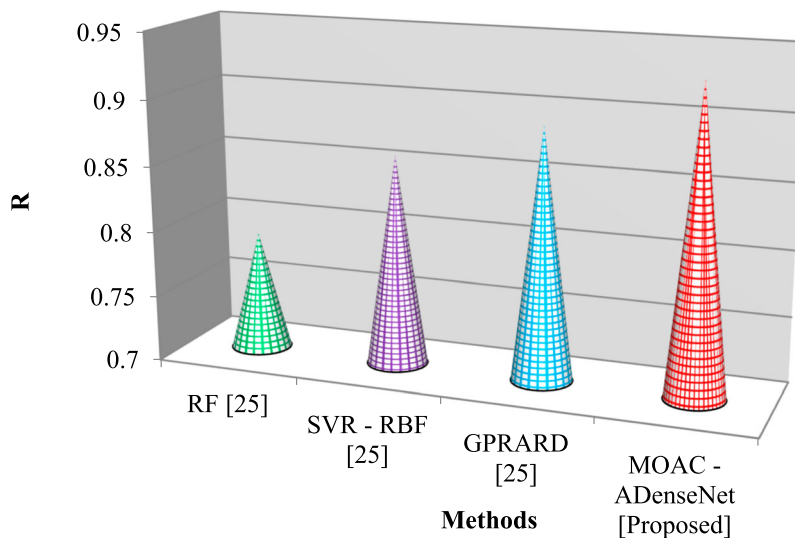


**Figure 8.** Graphical representation of R.

nonlinear correlations present in UHPC material characteristics and cost considerations. Furthermore, it can be difficult to determine the importance of individual variables for cost-effectiveness analysis due to their ensemble nature. GPRARD [31] is excellent in Bayesian optimization and uncertainty quantification, it can be computationally costly and necessitate extensive hyperparameter adjustment, which presents difficulties for large-scale UHPC material selection applications. Modelling nonlinear relationships with SVR-RBF [31] performs well, but selecting the right kernel values and regularization terms can be challenging. Furthermore, SVR-RBF might not function as well on very noisy or sparse data sets, which could make less useful in some UHPC material selection situations. However, they frequently have drawbacks like hardness in fine-tuning parameters, incapacity to manage big datasets and challenges in deciphering outcomes. The MOAC-ADenseNet technique has several benefits. By merging the capabilities of ant colony optimization and deep learning, it generates high-performance UHPC while efficiently optimizing several competing goals, including cost-effectiveness and sustainability. The shortcomings of current techniques are addressed by MOAC-ADenseNet, which can handle complicated, high-dimensional data with adaptability and scalability. This results in a thorough and understandable solution for economical UHPC material selection.

## 5. Conclusion

The study developed a MOAC-ADenseNet model with 5-K-Fold cross validation to address the inadequacies of traditional material selection methods in the manufacturing of HPC. The approach optimized material selection while taking performance, cost-effectiveness and sustainability factors are considered. With a strong Pearson's Linear Correlation Coefficient (R) and a low

Mean Absolute Percentage Error (MAPE), the method showed excellent precision and dependability in its ability to anticipate the HPC cost of materials. The results showed the efficiency of the MOAC-ADenseNet in enhancing material selection for UHPC manufacturing while achieving cost-effectiveness and sustainability requirements. However, one of the limitations may include the need for more testing and refinement under various real-world conditions. Future research should focus on expanding the model's applicability to broader scenarios and incorporating more criteria for carefully selecting materials in HPC production.

## Disclosure statement

No potential conflict of interest was reported by the author(s).

## Ethics approval and consent to participate

No participation of humans takes place in this implementation process.

## Human and animal rights

No violation of Human and Animal Rights is involved.

## Authorship contributions

All authors are contributed equally to this work.

## Data availability statement

Data sharing not applicable to this article as no datasets were generated or analyzed during the current study.

## References

- [1] Wang J, Kim YJ, Liu C. Deep learning for detection and characterization of cracking in ultra-high-performance concrete. *ACI Struct J.* 2023;120(3):3–15.

- [2] Díaz J, Gálvez JC, Alberti MG, et al. Achieving ultra-high-performance concrete by using packing models in combination with nanoadditives. *Nanomaterials*. 2021;11(6):1414. doi:10.3390/nano11061414
- [3] Yan P, Chen B, Afgan S, et al. Experimental research on ductility enhancement of ultra-high performance concrete incorporation with basalt fibre, polypropylene fibre and glass fibre. *Constr Build Mater*. 2021;279:122489. doi:10.1016/j.conbuildmat.2021.122489
- [4] Akeed MH, Qaidi S, Ahmed HU, et al. Ultra-high-performance fiber-reinforced concrete. Part IV: durability properties, cost assessment, applications, and challenges. *Case Stud Constr Mater*. 2022;17:e01271.
- [5] Pezeshkian M, Delnavaz A, Delnavaz M. Development of UHPC mixtures using natural zeolite and glass sand as replacements of silica fume and quartz sand. *Eur J Environ Civil Eng*. 2021;25(11):2023–2038. doi:10.1080/19648189.2019.1610074
- [6] Kim MK, Le HV, Kim DJ. Electromechanical response of smart ultra-high performance concrete under external loads corresponding to different electrical measurements. *Sensors*. 2021;21(4):1281. doi:10.3390/s21041281
- [7] Dong S, Ding S, Han B, et al. Multifunctional super-fine stainless wires reinforced UHPC for smart prefabricated structures. In: Rizzo P, Milazzo A., editors. *European workshop on structural health monitoring*. EWSHM 2022. *Lecture Notes in Civil Engineering*, vol 253. Cham: Springer International Publishing; 2022 June. p. 794–804.
- [8] Le HV, Kim MK, Kim SU, et al. Enhancing self-stress sensing ability of smart ultra-high performance concretes under compression by using nano functional fillers. *J Build Eng*. 2021;44:102717. doi:10.1016/j.job.2021.102717
- [9] Akhnouk AK, Buckhalter C. Ultra-high-performance concrete: constituents, mechanical properties, applications and current challenges. *Case Stud Constr Mater*. 2021;15:e00559. doi:10.1016/j.cscm.2021.e00559
- [10] Tavares C, Skillen K, Shi X, et al. Multi-criteria comparison tools to evaluate cost-and eco-efficiency of ultra-high-performance concrete. *Environ Res Infrastruct Sustainability*. 2023;3(2):025010. doi:10.1088/2634-4505/acd475
- [11] Cao Y, Zhao P, Chen H, et al. Application of hybrid intelligent algorithm for multi-objective optimization of high-performance concrete in complex alpine environment highway. *Constr Build Mater*. 2023;406:133376. doi:10.1016/j.conbuildmat.2023.133376
- [12] Fan D, Yu R, Fu S, et al. Precise design and characteristics prediction of ultra-high-performance concrete (UHPC) based on artificial intelligence techniques. *Cem Concr Compos*. 2021;122:104171. doi:10.1016/j.cemconcomp.2021.104171
- [13] Beskopylny AN, Stel'makh SA, Shcherban EM, et al. Developing environmentally sustainable and cost-effective geopolymer concrete with improved characteristics. *Sustainability*. 2021;13(24):13607. doi:10.3390/su132413607
- [14] Chen H, Deng T, Du T, et al. An RF and LSSVM–NSGA-II method for the multi-objective optimization of high-performance concrete durability. *Cem Concr Compos*. 2022;129:104446. doi:10.1016/j.cemconcomp.2022.104446
- [15] Mahjoubi S, Barhemat R, Meng W, et al. AI-guided auto-discovery of low-carbon cost-effective ultra-high-performance concrete (UHPC). *Resour Conserv Recycl*. 2023;189:106741. doi:10.1016/j.resconrec.2022.106741
- [16] Guo P, Mahjoubi S, Liu K, et al. Self-updatable AI-assisted design of low-carbon cost-effective ultra-high-performance concrete (UHPC). *Case Stud Constr Mater*. 2023;19:e02625.
- [17] Qin X, Kaewunruen S. Eco-friendly design and sustainability assessments of fibre-reinforced high-strength concrete structures automated by data-driven machine learning models. *Sustainability*. 2023;15(8):6640. doi:10.3390/su15086640
- [18] Sun C, Wang K, Liu Q, et al. Machine-learning-based comprehensive properties prediction and mixture design optimization of ultra-high-performance concrete. *Sustainability*. 2023;15(21):15338. doi:10.3390/su152115338
- [19] Tavares C Sarmiento Goncalves Martins E (2022). Multi-objective density diagrams developed with machine learning models to optimize sustainability and cost-efficiency of UHPC mix design [doctoral dissertation].
- [20] Mahjoubi S, Bao Y, Meng W, et al. AI-guided auto-discovery of low-carbon cost-effective ultra-high-performance concrete: data synthesis, semi-supervised learning, and many-objective optimization. In: *International interactive symposium on ultra-high-performance concrete*. Vol. 3, No. 1. Iowa State University Digital Press; 2023 June. p. 106741.
- [21] Makul N. Advanced smart concrete-A review of current progress, benefits and challenges. *J Cleaner Prod*. 2020;274:122899. doi:10.1016/j.jclepro.2020.122899
- [22] Shah KW, Huseien GF. Biomimetic self-healing cementitious construction materials for smart buildings. *Biomimetics*. 2020;5(4):47. doi:10.3390/biomimetics5040047
- [23] Abellan-Garcia J. Study of nonlinear relationships between dosage mixture design and the compressive strength of UHPC. *Case Stud Constr Mater*. 2022;17:e01228.
- [24] Kalaivani K, Kshirsagar PR, Sirisha Devi J, et al. Prediction of biomedical signals using deep learning techniques. *J Intell Fuzzy Syst*. 2023;44(6):9769–9782. doi:10.3233/JIFS-230399
- [25] Chiranjeevi P, Rajaram A. A lightweight deep learning model based recommender system by sentiment analysis. *J Intell Fuzzy Syst*. 2023;44(6):10537–10550. doi:10.3233/JIFS-223871
- [26] Babu PA, Rai AK, Ramesh JVN, et al. An explainable deep learning approach for oral cancer detection. *J Electr Eng Technol*. 2024;19(3):1837–1848. doi:10.1007/s42835-023-01654-1
- [27] Pradeep J, Raja Ratna S, Dhal PK, et al. Deepfore: a deep reinforcement learning approach for power forecasting in renewable energy systems. *Electr Power Compon Syst*. 2024: 1–17. doi:10.1080/15325008.2024.2332391
- [28] Niu Y, Wang W, Su Y, et al. Plastic damage prediction of concrete under compression based on deep learning. *Acta Mech*. 2024;235(1):255–266. doi:10.1007/s00707-023-03743-8
- [29] Zekrif DMS, Dhanalakshmi M, Puviarasi R, et al. Optimized controller design for renewable energy systems by using deep reinforcement learning technique. *Int J Renew Energy Res (IJRER)*. 2024;14(1):101–110.
- [30] Long X, Mao MH, Su TX, et al. Machine learning method to predict dynamic compressive response of

- concrete-like material at high strain rates. *Def Technol.* **2023**;23:100–111. doi:[10.1016/j.dt.2022.02.003](https://doi.org/10.1016/j.dt.2022.02.003)
- [31] Kovačević M, Ivanišević N, Petronijević P, et al. Construction cost estimation of reinforced and prestressed concrete bridges using machine learning. *Građevinar.* **2021**;73(01):1–13.
- [32] Song X, Wang W, Deng Y, et al. Data-driven modeling for residual velocity of projectile penetrating reinforced concrete slabs. *Eng Struct.* **2024**;306:117761. doi:[10.1016/j.engstruct.2024.117761](https://doi.org/10.1016/j.engstruct.2024.117761)
- [33] Long X, Li H, Iyela PM, et al. Predicting the bond stress–slip behavior of steel reinforcement in concrete under static and dynamic loadings by finite element, deep learning and analytical methods. *Eng Fail Anal.* **2024**;161:108312. doi:[10.1016/j.engfailanal.2024.108312](https://doi.org/10.1016/j.engfailanal.2024.108312)
- [34] Lian J, Wang Y, Fu T, et al. Mechanical, electrical, and tensile self-sensing properties of ultra-high-performance concrete enhanced with sugarcane bagasse Ash. *Materials (Basel).* **2023**;17(1):82. doi:[10.3390/ma17010082](https://doi.org/10.3390/ma17010082)